Origin of Long-Range Ferromagnetic Ordering in Metal−Organic Frameworks with Antiferromagnetic Dimeric-Cu(II) Building Units

Lei Shen,[†,‡] Shuo-Wang Yang,*[,‡] Shengchang Xiang,[§] Tao Liu,[‖] Bangchuan Zhao,[⊥,⊗] Man-Fai Ng,[‡] Jörg Göettlicher,[‖] Jiabao Yi,*[,¶] Sean Li,[¶] Lan Wang,[⊥] Jun Ding,[#] Banglin Chen,[§] Su-Huai Wei,[+] and Yuan Ping Feng*[,†]

[†]Department of Physics, 2 Science Drive 3, National University of Singapore, Singapore 117542, Singapore

[‡]Institute of High Performance Computing, Agency for Science, Technology and Research, 1 Fusionopolis Way, #16-16 Connexis, Singapore 138632, Singapore

[§]Department of Chemistry, University of Texas at San Antonio, One UTSA Circle, San Antonio, Texas 78249-1640, United States

[‖]Institute for Synchrotron Radiation, Karlsruhe Institute of Technology, 76344 Eggenstein-Leopoldshafen, Germany

[⊥]Division of Physics and Applied Physics, School of Physical and Mathematical Sciences, Nanyang Technological University, 21 Nanyang Link, Singapore 637371, Singapore

[⊗]Institute of Solid State Physics, Chinese Academy of Sciences, Shushan Lake Road 350# Hefei, Anhui, China 230031

[¶]Department of Materials Science and Engineering, National University of Singapore, Singapore 117576, Singapore

[#]Schools of Materials Science and Engineering, University of New South Wales, 2052 New South Wales, Australia

[+]National Renewable Energy Laboratory, Golden, Colorado 80401-3393, United States

S *Supporting Information*

ABSTRACT: Even though metal−organic frameworks (MOFs) derived from antiferromagnetic dimeric-Cu(II) building units and nonmagnetic molecular linkers are known to exhibit unexpected ferromagnetic behavior, a comprehensive understanding of the underlying mechanism remains elusive. Using a combined theoretical and experimental approach, here we reveal the origin of the long-range ferromagnetic coupling in a series of MOFs, constructed from antiferromagnetic dimeric-Cu(II) building blocks. Our studies show that the strong localization of copper vacancy states favors spontaneous spin polarization and formation of local moment. These copper vacancy-induced moments are coupled via the itinerant electrons in the conjugated aromatic linkers to establish a long-range ferromagnetic ordering. The proposed mechanism is supported by direct experimental evidence of copper vacancies and the magnetic hysteresis (M-H) loops.
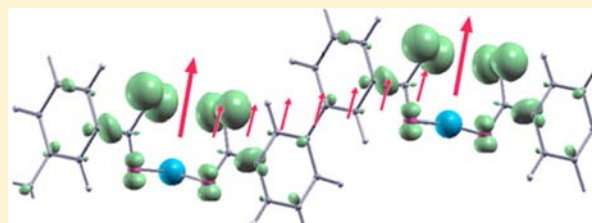
INTRODUCTION

Metal−organic frameworks (MOFs) are porous network structures consisting of metal oxide clusters linked by molecular chains. This new class of materials shows promising applications in gas storage,[1] luminescent detectors,[2] molecular sieves,[3] drug delivery,[4] and catalysis.[5] Meanwhile, many MOFs exhibit unique magnetic properties due to constitutive open-shell transition metal ions, which has been attracting much attention[6−10] because of their potential applications in low density magnetic biomedicine, molecular magnets, and magnetic molecular sensors. Understanding and chemically controlling the magnetic properties of these materials remains a key challenge. The magnetic properties of MOFs are mainly attributed to metal ions with unpaired electrons, and Co^{2+}/Co^{3+}, Fe^{2+}/Fe^{3+} and Cu^{2+} containing MOFs have been widely studied for their magnetic properties.[1−3,6,9] Because of the strong superexchange coupling between two Cu(II) ions within a paddle-wheel $Cu_2(COO)_4$, the secondary building unit

containing a Cu(II) dimer (Cu_2−SBUs, Figure 1a) has antiferromagnetic (AFM) spin alignment with zero total magnetic moment.[11] Thus, Cu_2−SBUs constructed MOFs are not expected to exhibit ferromagnetic (FM) features as observed for MOF-11 (1) with PtS topology.[12] However, Williams et al. observed, for the first time, a FM feature in a three-dimensional (3D) Cu_2−SBU constructed MOF, HKUST-1 (2), with a Curie temperature (T_C) of 4.7 K.[6] Later, Zaworotko et al. discovered structural dependent magnetic properties in Cu_2(m-BDC)$_2$ (m-BDC = 1,3-Benzenedicarboxylate) polymorphs.[8] They found that triangularly arranged Cu_2(m-BDC)$_2$ framework (3,3 Δ) shows FM feature at 5 K, while at the same temperature, the Cu_2(m-BDC)$_2$ framework of square lattice (4,4 □) does not. It is speculated that the different magnetic properties of the two
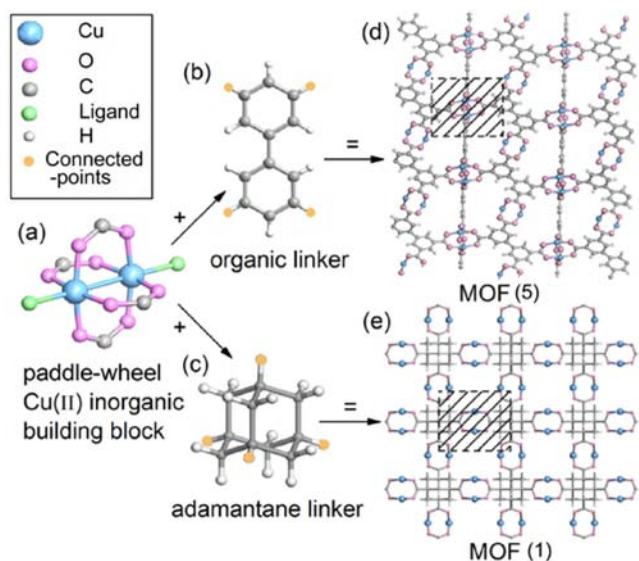
Figure 1. (a) A basic "paddle-wheel" $Cu_2(COO)_4$ metal ions-containing secondary building unit (Cu_2−SBU); (b) rigid aromatic and (c) adamantane linkers, respectively; Schematic structural constructions of (d) MOF (5) (see detail linkers and structures of MOF(2−4) in Supporting Information, Figure S2) and (e) MOF (1), respectively. All MOFs have the Cu_2−SBU + aromatic/adamantane linkers. The enlarged shadow areas are shown in Figure 2a,b.

RESULTS AND DISCUSSION

In ionic crystals of vacancy-induced magnetism, cationic vacancies favor the formation of local moments compared to anionic vacancies due to the localized cationic vacancy wave functions.[15] At first, we consider a single V_{Cu} which is simulated by removing a Cu(II) ion from the supercell. Introducing the V_{Cu} breaks the spin dimer. Taking MOF (5) as an example, our calculations predict that a single V_{Cu} favors a spin-polarized state with a spin-polarization energy of 199 meV. Such strong spin polarization results in a complete separation of the majority and minority states and the formation of a local moment of 0.73 μ_B. We also calculate the C and O atomic vacancies in MOF (5) and find no formation of local magnetic moments, which is in good agreement with vacancy-induced magnetism in semiconductors.[15] The localization of the magnetic moments of V_{Cu} can also be visualized by plotting the defect state charge density in the real space. For example, Figure 2c,d shows the evidence that these defect states are
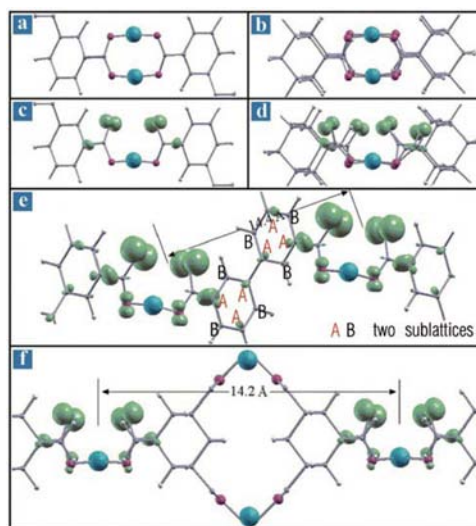

Figure 2. (a and b) are enlarged shadow areas of panels (d) and (e) in Figure 1, respectively, which are perfect single crystal without defects; (c) and (e) show the spin densities of MOF (5) with a single copper vacancy and a pair of copper vacancies, respectively. (d) and (f) show the same situations for MOF (1). The distance between the two vacancies is indicated. The isovalues are 0.03 e/Å^3.

aforementioned Cu_2(m-BDC)$_2$ MOFs are due to the spin frustration in the triangular arrangement of Cu_2−SBUs.[8] Veciana et al. questioned such a hypothesis because a net spin is needed on each node to cause the spin frustration but the AFM Cu_2−SBU does not possess a net spin.[13] Theoretical calculations indicated that, in order to generate a net spin and subsequent spin frustration in an AFM Cu_2−SBU, a minimal spin-flip energy of 630 meV is required [see Supporting Information, Figure S1]. Such a high energy barrier is impossible to overcome at 5 K. Therefore, there remain two mysteries, how the strongly AFM coupled Cu_2−SBUs can generate a local magnetic moment and how these moments can be coupled over a large distance (~9.5 Å in HKUST-1 which is the minimum separation of the Cu_2−SBUs).

Motivated by vacancy induced magnetism in many materials such as graphene[14] and dilute magnetic semiconductors (DMSs),[15] we investigate the possibility of ferromagnetism induced by point defects, that is, Cu vacancy (V_{Cu}), in a series of Cu_2−SBU based MOFs. The other defects, such as atomic C and O vacancies, are also calculated, but they cannot induce any magnetic moment due to the delocalization of their defect wave functions.[15] Magnetic properties of five MOFs (1−5) listed in Table 1 were investigated theoretically. Moreover, experimental studies were carried out on one of them, MOF-505 (5),[16] in order to validate our theoretical predictions. On the basis of our density functional theory (DFT) calculations on these five MOFs and experimental observations on MOF (5), we conclude that the magnetic moments in these MOFs are originated from V_{Cu}, which breaks the balance of the AFM state in Cu_2−SBUs and creates quasi-localized spin states of 2p orbital on oxygen (O) and carbon (C) atoms around it. These quasi-localized spin states are FM coupled via itinerant π electrons in the conjugated aromatic linkers (Figure 1b).

strongly localized on the oxygen atoms surrounding the V_{Cu} in MOF (5) and MOF (1), not on the another Cu atom in the same dimer. This is because of the strong localization of copper defect wave functions.[15] The formation energy of a single V_{Cu} can vary from 2.50 eV under Cu-rich condition to −0.44 eV under Cu-poor condition (see Supporting Information Figure S3), depending on the synthesis conditions. The negative formation energy under Cu-poor condition implies spontaneous formation of V_{Cu}. Furthermore, vacancies are inevitable especially for large organic-metal complex systems such as MOFs during the chemical fabrication processes.[16] It is difficult to obtain samples with well-defined vacancy concentrations as well as perfect crystal, but we still can provide direct evidence of V_{Cu} in the synthesized MOF (5). We fabricated MOF (5) following the same method described in ref 16, and measured the extended X-ray absorption fine structure (EXAFS) spectrum at the Cu K-edge. By comparing the spectrum of MOF (5) with a relatively good crystal CuAc$_2$ sample (Figure

3a), we found that the Cu—O distance of the first shell is 1.95 Å, but the second Cu—Cu ordering peak is absent. In contrast,
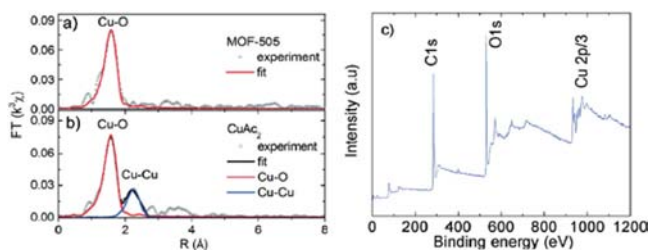

Figure 3. (a) Fourier transform of the EXAFS at Cu K-edge of synthesized MOF (5), the first peak was fitted by Cu—O coordination; (b) Fourier transform of the EXAFS of $CuAc_2$ at Cu K-edge, indicating the coordination for both the first Cu—O and the second Cu—Cu ordering shells. The two shells were fitted by theoretical phase-shift extracted from crystallographic data. (c) Wide scan XPS spectrum of MOF (5).

a Cu—Cu ordering peak can be clearly seen in $CuAc_2$ sample with a distance of 2.58 Å (Figure 3b). Both MOF (5) and $CuAc_2$ samples possess similar Cu—Cu coordination in the second shell[17] and the measurements were carried out under the same condition. The missing Cu—Cu peak in the EXAFS spectrum of MOF (5) is very likely due to the formation of Cu vacancies.

In addition, X-ray photoelectron spectroscopy (XPS) was used to examine the composition of MOF (5), after the sample was annealed for 2 h at 400 K to remove possible adsorbed water molecules. On the basis of XPS spectrum in Figure 3c, we deduce a Cu/O ratio of 1:11.6 for our synthesized MOF (5), which is lower than that in MOF (5) with and without crystallized water, 1:10 and 1:7 respectively. This further suggests the existence of Cu vacancies. Moreover, based on the XPS results, the concentration of atomic Cu vacancies in the crystal surface of MOF (5) is estimated to be around 1.04%. It is noted that the XPS spectrum only shows the surface chemical environment. Therefore, our calculated V_{Cu} concentration is not for bulk crystal. The bulk V_{Cu} concentration should be much lower than 1.04%. Therefore, we also use Energy-dispersive X-ray spectroscopy (EDS) attached SEM system to evaluate the composition of this sample. It is found that the Cu/O ratio is approximately 1:9, which corresponds to a Cu vacancy of 0.57%. Although we cannot provide very accurate V_{Cu} concentration in the synthesized MOF (5), we can confirm the existence of Cu vacancy in MOF (5) based on the three aforementioned analytical methods.

The spin densities of MOF (5) and MOF (1) with a single V_{Cu} each are shown in Figure 2, panels c and d, respectively. It is seen that V_{Cu} does generate defect spin states in both MOFs. These defects spin states show p-orbital characteristics and are mainly localized on oxygen and carbon atoms which are neighbors of V_{Cu}. Remarkably, this is very similar to the cationic vacancy-induced FM in DMSs, which is due to the electron redistribution after removing cations.[15] Our calculations indicate that V_{Cu} in Cu_2—SBUs is responsible for the net spin states, and it is the origin of the local magnetic moments in these two MOFs. Similar results were obtained for other MOFs being studied.

As we know, the existence of local moments does not necessarily result in collective magnetism. Therefore, after identifying the origin of the local magnetic moments in MOFs,

the next issue is whether the moments are coupled ferromagnetically or antiferromagnetically, long-range or short-range. A long-range ferromagnetic coupling is critical for achieving high temperature ferromagnetism at low defect concentrations, such as in MOFs. Different from those in dilute magnetic semiconductors (DMSs), defect states in MOFs are localized in regions separated by at least 14 Å, and such a long-range FM coupling cannot be mediated by simple super-exchange interaction involving either 2p orbitals of O or C atoms, or 3d orbital of Cu ions because of their localized special distribution of wave functions (see Supporting Information, Figure S4).[15] Furthermore, the common types of ferromagnetic mechanism are excluded in Cu(II)-MOFs (see Supporting Information Section IV and Figure S4). Recently, it was proposed that the delocalized π electrons in graphene are able to mediate spin coupling over a long-range in the defect-induced "Stoner" magnetism, where the coupling distance between the local moments induced by carbon vacancies can reach as large as 20 Å in graphene through the Ruderman-Kittel-Kasuya-Yosida (RKKY)-like interaction.[14,18] In MOF (5), the Cu_2—SBUs are linked by biphenyl (BP) which has conjugated π electrons similar to that in graphene. It is thus reasonable to speculate that the long-range FM coupling between the V_{Cu} induced defect spin states could be mediated by these delocalized itinerant π electrons in the BP linkers.

To verify such a hypothesis, we calculated the magnetic property of two copper vacancies located in neighboring Cu_2—SBUs which are modeled by removing one Cu(II) ion from each of the two neighboring Cu_2—SBUs in the aforementioned MOFs. We note that due to the unique structure of MOFs, FM coupling can be established at very low defect concentration. Taking again MOF (5) as an example, each Cu(II) building unit has 12 neighboring Cu(II) building units directly connected by the BP linkers. Theoretically, the minimum concentration of V_{Cu} required to have two copper vacancies directly connected by one BP linker in MOF (5) is much less than 1% (see Supporting Information, Figure S5). This implies that the copper vacancies can be in the coupling range even at very low concentration, which is in good agreement with our above experiment. As a matter of fact, it has been reported that a defect concentration of 1% is sufficient to generate detectable long-range FM ordering in diluted magnetic semiconductors at room temperature.[15]

The calculated results for all five MOFs being studied, including energy difference (ΔE) between the parallel and the antiparallel spin configurations, the distance between two neighboring V_{Cu}, and the induced magnetic moment are given in Table 1. Available experimental Curie temperatures (T_C) are also listed in the table. We compare the results of MOF (1) and MOF (5) first. The two V_{Cu} in these two MOFs have similar separations, that is, 14.2 Å in MOF (1) and 14.4 Å in MOF (5) (Figure 2e,f). The linker in MOF (5) is BP, an aromatic organic chain with delocalized π electrons (Figure 1b) but in MOF (1) is adamantine (ATC) that does not have delocalized electrons (Figure 1c). On the basis of the above hypothesis, FM coupling is expected in MOF (5) but not in MOF (1).[16]

In addition, the results of our calculations have confirmed that MOF (5) favors FM coupling, with a magnetic moment of 1.71 μ_B per pair of copper vacancies, and the energy of the FM state is 59 meV lower than that of the AFM state (Table 1). In contrast, the FM and AFM states of MOF (1) have comparable energies, suggesting weak magnetic interaction between the two copper vacancies (Figure 2f). These results are consistent with

Table 1. Calculated Magnetic Properties of Two Neighboring V_{Cu} Defects among Five Cu_2−SBU Constructed MOFs and Some Experimentally Observed Currie Temperature $(T_C)^a$

MOF	configuration	linker	ΔE (meV)	d (Å)	n (%)	MM (μ_B)	T_c (K)
1	MOF-11	ATC	0	14.2	3.00	0	0
2	HKUST-1	TMA^b	−40	9.5	3.64	1.80	4.7^c
3	$Cu_2(m\text{-}BDC)_2(\triangle)$	m-BDC	−82	8.0	2.78	2.00	$>5^d$
4	$Cu_2(m\text{-}BDC)_2(\square)$	m-BDC	−32	13.8	2.10	1.79	$<4.7^e$
5	MOF-505	BP	−59	14.4	1.52	1.71	11

$^a\Delta E = E_{FM} - E_{AFM}$, where E_{FM} and E_{AFM} are energies of the FM and AFM states, respectively. d is the distance between the two vacancies, n is calculated concentration of V_{Cu} based on MOFs' formulations, MM is the magnetic moment. ^{b}1,3,5-benzenetricarboxylate. ^{c}Ref 6. ^{d}Ref 8. ^{e}The value is a theoretical prediction based on the ΔE.

Figure 4. (a) Magnetic hysteresis loop of MOF (5) at 5 and 20 K, respectively; (b) temperature dependent susceptibility of MOF (5). The inset shows the $1/\chi - T$ curve in the temperature ranged from 2 to 65 K. The solid line in the inset is the curve fitted to the Curie−Weiss law.

the experimental observation.[6] It is noted that the aromatic linkers have graphene-like two sublattices and the spin states in MOF (5) are localized on the same sublattice of the aromatic linkers only, as shown in Figure 2e. This results in ferromagnetic coupling without a RKKY-like oscillating behavior.

The proposed mechanism also provides an explanation on why MOFs having the same building block can show completely different magnetic properties. It is the itinerant electrons in the linker that play a key role in the long-range magnetic coupling. Besides MOF (5) and MOF (1), our calculations suggest that the remaining three MOFs (2−4) all show FM coupling (Table 1). The only difference of the ferromagnetic behavior between them is their different Curie temperature. This is because the linkers in these structures (TMA and m-BDC) are also conjugated chains with delocalized π electrons, similar to the BP linkers in MOF (5). Of the four FM MOFs, MOF (4) has the smallest energy difference between the FM and AFM states ($\Delta E = -32$ meV). Compared to other FM MOFs, a lower T_C is expected for MOF (4) due to the weaker FM coupling between the copper vacancies. In comparison, MOF (2) shows a large energy difference ($\Delta E = -40$ meV) and a much shorter vacancy separation (9.5 Å). Since the T_C of MOF (2) is 4.7 K, MOF (4) is expected to have a ferromagnetic ordering temperature lower than 4.7 K, which could be the reason why MOF (4)'s FM feature is not observed at 5 K.[8] The distance between two Cu vacancies is related to the concentration of V_{Cu} if the doping is uniform in experiment. Therefore, the calculated reference values of concentration of V_{Cu} are also listed in Table 1.

To provide further support to the proposed mechanism, we measured the magnetic-hysteresis (M-H) loops for MOF (5) at 5 and 20 K, respectively, and show the results in Figure 4a. A well-defined M-H loop can be seen at 5 K, indicating ferromagnetic ordering in the sample. Furthermore, we measured the temperature dependency susceptibility to obtain the Curie temperature. The result is shown in Figure 4b, where the inset shows the inverse susceptibility. By fitting the data to the Curie−Weiss law, a T_C of 11 K is obtained for MOF (5), which is higher than that of MOF (2) (4.7 K), as expected. It is worth pointing out that the organic molecular linker in MOF (5) is different from a usual biphenyl group. Due to the constraint in the network structure, the biphenyl group in MOF (5) has a planar structure which is an excellent conjugated
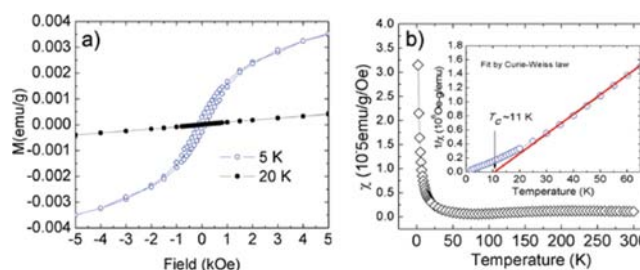
system providing effective mediation of ferromagnetism originated from V_{Cu}. This unique structural advantage could be the reason for the higher Curie temperature of MOF (5) compared to that of substituted benzenecarboxylate conjugated systems such as that in MOF (2).

CONCLUSIONS

In summary, based on the DFT calculated magnetic properties of a series of MOFs (1−5) and experimental investigations on MOF (5), we elucidated why some AFM Cu_2−SBUs constructed MOFs exhibit FM features, and identified Cu vacancies as the origin of localized spin states and local moments. The collective long-range ferromagnetism is due to the coupling between these localized spin states via delocalized π electrons in conjugated aromatic linkers. The copper defect states and itinerant π electrons in the linkers play the key role in long-range ferromagnetism in Cu_2−SBUs based MOFs. The proposed mechanism is confirmed by direct experimental evidence of copper vacancies and long-range collective ferromagnetism in MOF (5). This mechanism is expected to be general and can hold in a diverse range of Cu_2−SBUs based MOFs.

In addition, our work demonstrated that it is possible to make use of the rich organic chemistry to construct highly conjugated aromatic linkers that provide magnetic coupling between the V_{Cu} induced magnetic moments to obtain ferromagnetism. In fact, organic linkers containing aromatic units have been recently assembled into highly porous Cu_2−SBUs based MOFs.[19] Our work has highlighted the bright promise of such Cu_2−SBUs based MOFs as excellent novel FM porous materials. The understanding of the long-range ferromagnetic ordering materials is valuable in further exploration of this wide class of materials and in designing new high T_C Cu_2−SBUs based FM MOFs.

ASSOCIATED CONTENT

S Supporting Information
Theoretical calculation method, formation energy calculations, experimental details, spin flipping energy, radial charge distribution and details of MOF optimized structures. This material is available free of charge via the Internet at http://pubs.acs.org.

AUTHOR INFORMATION

Corresponding Author
yangsw@ihpc.a-star.edu.sg; jiabao.yi@unsw.edu.au; phfyp@nus.edu.sg

Notes

The authors declare no competing financial interest.

■ REFERENCES

(1) (a) Chen, B.; Eddaoudi, M.; Hyde, S. T.; Keeffe, M. O.; Yaghi, O. M. *Science* **2001**, *291*, 1021. (b) Seayad, A. M.; Antonelli, D. M. *Adv. Mater.* **2004**, *16*, 756. (c) Dinca, M.; Han, W. S.; Liu, Y.; Dailly, A.; Brown, C. M.; Long, J. R. *Angew. Chem., Int. Ed.* **2007**, *46*, 1419. (d) Lin, X.; Jia, J.; Zhao, X.; Thomas, K. M.; Blake, A. J.; Walker, G. S.; Champness, N. R.; Hubberstey, P.; Schroder, M. *Angew. Chem., Int. Ed.* **2006**, *45*, 7358. (e) Collins, D. J.; Zhou, H.-C. *J. Mater. Chem.* **2007**, *17*, 3154. (f) Dinca, M.; Dailly, A.; Liu, Y.; Brown, C. M.; Neumann, D. A.; Long, J. R. *J. Am. Chem. Soc.* **2006**, *128*, 16876. (g) Latroche, M; Surble, S.; Serre, C.; Mellot-Draznieks, C; Llewellyn, P. L.; Lee, J.-H.; Chang, J.-S.; Jhung, S. H.; Ferey, G. *Angew. Chem., Int. Ed.* **2006**, *45*, 8227. (h) Pan, L.; Sander, M. B.; Huang, X. Y.; Li, J.; Smith, M.; Bittner, E.; Bockrath, B.; Johnson, J. K. *J. Am. Chem. Soc.* **2004**, *126*, 1308. (i) Ma, S. Q.; Sun, D. F.; Simmons, J. M.; Collier, C. D.; Yuan, D. Q.; Zhou, H.-C. *J. Am. Chem. Soc.* **2008**, *130*, 1012. (j) Rosenbach, N.; Jobic, H.; Ghoufi, A.; Salles, F.; Maurin, G.; Bourrelly, S.; Llewellyn, P. L.; Devic, T.; Serre, C.; Ferey, G. *Angew. Chem., Int. Ed.* **2008**, *47*, 6611.

(2) (a) Chen, B.; Wang, L.; Xiao, Y.; Fronczek, F. R.; Xue, M.; Cui, Y.; Qian, G. *Angew. Chem., Int. Ed.* **2009**, *48*, 500. (b) Chen, B.; Wang, L.; Zapata, F.; Qian, G.; Lobkovsky, E. B. *J. Am. Chem. Soc.* **2008**, *130*, 6718. (c) Chen, B.; Yang, Y.; Zapata, F.; Lin, G.; Qian, G.; Lobkovsky, E. B. *J. Am. Chem. Soc.* **2007**, *129*, 1693.

(3) (a) Chen, B.; Liang, C.; Yang, J.; Contreras, D. S.; Clancy, Y. L.; Lobkovsky, E. B.; Yaghi, O. M.; Dai, S. *Angew. Chem., Int. Ed.* **2006**, *45*, 1390. (b) Salles, F.; Ghoufi, A.; Maurin, G.; Bell, R. G.; Mellot-Draznieks, C; Ferey, G. *Angew. Chem., Int. Ed.* **2008**, *47*, 8487. (c) Pan, L.; Olson, D. H.; Ciemnolonski, L. R.; Heddy, R.; Li, J. *Angew. Chem., Int. Ed.* **2006**, *45*, 616. (d) Dybtsev, D. N.; Chun, H.; Kim, K. *Angew. Chem., Int. Ed.* **2004**, *46*, 5033. (e) Ma, S. Q.; Sun, D. F.; Wang, X. S.; Zhou, H. C. *Angew. Chem., Int. Ed.* **2007**, *46*, 2458. (f) Chen, B.; Ma, S.; Zapata, F.; Fronczek, F. R.; Lobkovsky, E. B.; Zhou, H. C. *Inorg. Chem.* **2007**, *46*, 1233.

(4) Horcajada, P.; Serre, C.; Vallet-Regi, M.; Sebban, M.; Taulelle, F.; Ferey, G. *Angew. Chem., Int. Ed.* **2006**, *45*, 5974.

(5) (a) Corma, A. *Chem. Rev.* **1995**, *95*, 559. (b) Kitagawa, S.; Kitaura, R.; Noro, S. *Angew. Chem., Int. Ed.* **2004**, *43*, 2334.

(6) (a) Chui, S. S.-Y.; Lo, S. M. F.; Charmant, J. P. H.; Orpen, A. G.; Williams, I. D. *Science* **1999**, *283*, 1184. (b) Zhang, X. X.; Chui, S. S.-Y.; Williams, I. D. *J. Appl. Phys.* **2000**, *87*, 6007.

(7) (a) Zheng, Y. Z.; Tong, M. L.; Xue, W.; Zhang, W. X.; Chen, X. M.; Grandjean, F.; Long, G. J. *Angew. Chem., Int. Ed.* **2007**, *46*, 6076. (b) Zeng, M. H.; Yao, M. X.; Liang, H.; Zhang, W. X.; Chen, X. M. *Angew. Chem., Int. Ed.* **2007**, *46*, 1832.

(8) Moulton, B.; Lu, J.; Hajndl, R.; Hariharan, S.; Zaworotko, M. J. *Angew. Chem., Int. Ed.* **2002**, *41*, 2821.

(9) (a) Xiang, S. C.; Wu, X. T.; Zhang, J. J.; Fu, R. B.; Hu, S. M.; Zhang, X. D. *J. Am. Chem. Soc.* **2005**, *127*, 16352. (b) Xiang, S. C.; Hu, S. M.; Sheng, T. L.; Fu, R. B.; Wu, X. T.; Zhang, X. D. *J. Am. Chem. Soc.* **2007**, *129*, 15144.

(10) Sun, Y. Y.; Kim, Y.-K.; Zhang, S. B. *J. Am. Chem. Soc.* **2007**, *129*, 12606.

(11) (a) Kahn, O. *Molecular Magnetism*, 1st ed.; VCH: Cambridge, 1993; p 105; (b) Rodriguez-Fortea, A.; Alemany, P.; Alvarez, S.; Ruiz, E. *Chem.—Eur. J.* **2001**, *7*, 627.

(12) Chen, B.; Eddaoudi, M.; Reineke, T. M.; Kampf, J. W.; O'Keeffe, M.; Yaghi, O. M. *J. Am. Chem. Soc.* **2000**, *122*, 11559.

(13) Maspoch, D.; Ruiz-Molina, D.; Veciana, J. *Chem. Soc. Rev.* **2007**, *36*, 770−818.

(14) (a) Pisani, L.; Montanari, B.; Harrison, N. M. *New J. Phys.* **2008**, *10*, 033002. (b) Yazyev, O. V.; Helm, L. *Phys. Rev. B* **2007**, *75*, 125408−125411. (c) Osorio-Guillen, J.; Lany, S.; Barabash, S. V.; Zunger, A. *Phys. Rev. Lett.* **2006**, *96*, 107203−107206. (d) Palacios, J. J.; Fernandez-Rossier, J.; Brey, L. *Phys. Rev. B* **2008**, *77*, 195428−195441.

(15) (a) Dev, P.; Xue, Y.; Zhang, P. H. *Phys. Rev. Lett.* **2008**, *100*, 117204. (b) Pan, H.; Yi, J. B.; Shen, L.; Wu, R. Q.; Yang, J. H.; Lin, J. Y.; Feng, Y. P.; Ding, J.; Van, L. H.; Yin, J. H. *Phys. Rev. Lett.* **2007**, *99*, 127201. (c) Yi, J. B.; Lim, C. C.; Xing, G. Z.; Fan, H. M.; Van, L. H.; Huang, S. L.; Yang, K. S.; Huang, X. L.; Qin, X. B.; Wang, B. Y.; Wu, T.; Wang, L.; Zhang, H. T.; Gao, X. Y.; Liu, T.; Wee, A. T. S.; Feng, Y. P.; Ding, J. *Phys. Rev. Lett.* **2010**, *104*, 137201. (d) Peng, H. W.; Xiang, H. J.; Wei, S.-H.; Li, S.-S.; Li, J.-B.; Xia, J. B.; Li, J. B. *Phys. Rev. Lett.* **2009**, *102*, 017201.

(16) Chen, B.; Ockwig, N. W.; Millward, A. R.; Contreras, D. S.; Yaghi, O. M. *Angew. Chem., Int. Ed.* **2005**, *44*, 4745.

(17) (a) van Niekerk, J. N.; Schoening, F. R. L. *Nature (London)* **1953**, *171*, 36. (b) Wells, A. F. *Structural Inorganic Chemistry*; Oxford: Clarendon Press: London, 1984.

(18) (a) Ruderman, M. A.; Kittel, C. *Phys. Rev.* **1954**, *96*, 99. Kasuya, T. *Prog. Theor. Phys.* **1956**, *16*, 45. (b) Yosida, K. *Phys. Rev.* **1957**, *106*, 893.

(19) (a) Ma, L.; Mihalcik, D. J.; Lin, W. *J. Am. Chem. Soc.* **2009**, *131*, 4610−4611. (b) Ma, L.; Mihalcik, D. J.; Lin, W. *Angew. Chem., Int. Ed.* **2009**, *48*, 3637−3640.

17290

dx.doi.org/10.1021/ja3077654 | *J. Am. Chem. Soc.* 2012, 134, 17286−17290